

- ing that a ≥ 20 m can yield "acceptable" pressures ≤ 30 MPa for the given amplitudes; however, this size is incompatible with other evidence, for example mineralogical constraints on magma ascent rate, and conduit flow modeling. The medium is inhomogeneous, with $\mu_{\text{lava}} < \mu_{\text{edifice}}$. Full resolution of the issue requires three-dimensional elastic-plastic modeling. Seismic threshold overpressures in the text are calculated by recalibrating the maximum amplitude pressure to 10 to 27 MPa, as deduced by R. E. A. Robertson *et al.* (2), and applying similar methods for the August explosions.
20. Shear resistance was calculated by assuming an extrusion overpressure of 10 to 27 MPa and setting it equal to shear strength times boundary area of plug. Plug depth was assumed as ~ 270 m. Weight of extruded magma is accounted for by definition of overpressure.
21. M. V. Stasiuk, C. Jaupart, and R. S. J. Sparks [*Earth Planet. Sci. Lett.* **114**, 505 (1993)] estimated initial excess chamber pressures of 10 to 23 MPa for lava eruptions at Lonquimay, Chile, in 1989; Soufriere, St. Vincent, in 1979; and Paracutin in 1946 to 1952. During strong tilt cycles, the outlet pressure may be augmented by the average of uppermost-conduit pressure variations.
22. J. D. Devine, M. J. Rutherford, J. E. Gardner *Geophys. Res. Lett.* **25**, 3673 (1998).
23. E. Rabinowicz, *Proc. Phys. Soc. (London)* **71**, 668 (1958).
24. P. Okubo and J. H. Dieterich, in *Earthquake Source Mechanics*, S. Das, J. Boatwright, C. Scholz, Eds. (American Geophysical Union, Washington, DC, 1986), pp. 25–36; C. H. Scholz, *The Mechanics of Earthquakes and Faulting*. (Cambridge Univ. Press, Cambridge, 1990).
25. Feedback between pressurization and flow from the chamber result in decline of flux as magma degasses

and stiffens, and gas pressure builds, followed by accelerated flux after pressure is relieved. For one set of constraints, the system may be stable and independent of velocity perturbation; for another, it may be stable under quasi-static loading but unstable if subjected to a large pressurization or velocity jump [J. R. Rice and A. L. Ruina, *J. Appl. Mech.* **105**, 343 (1983); J. C. Gu, J. R. Rice, A. L. Ruina, S. T. Tse, *J. Mech. Phys. Solids* **32**, 167 (1984)].

26. We thank our colleagues at Montserrat Volcano Observatory for assistance. Supported by the Department for International Development (UK), the British Geological Survey (BGS), the Seismic Research Unit of the University of the West Indies, and the U.S. Geological Survey (USGS). B.V. acknowledges support from NSF, BGS, and USGS, and R.S.J.S. from the Natural Environmental Research Council, and the Leverhulme Trust.

28 July 1998; accepted 7 January 1999

Cristobalite in Volcanic Ash of the Soufriere Hills Volcano, Montserrat, British West Indies

P. J. Baxter,¹ C. Bonadonna,² R. Dupree,³ V. L. Hards,⁴
S. C. Kohn,² M. D. Murphy,² A. Nichols,⁵ R. A. Nicholson,⁴
G. Norton,⁴ A. Searl,⁵ R. S. J. Sparks,^{2*} B. P. Vickers⁴

Crystalline silica (mostly cristobalite) was produced by vapor-phase crystallization and devitrification in the andesite lava dome of the Soufriere Hills volcano, Montserrat. The sub-10-micrometer fraction of ash generated by pyroclastic flows formed by lava dome collapse contains 10 to 24 weight percent crystalline silica, an enrichment of 2 to 5 relative to the magma caused by selective crushing of the groundmass. The sub-10-micrometer fraction of ash generated by explosive eruptions has much lower contents (3 to 6 percent) of crystalline silica. High levels of cristobalite in respirable ash raise concerns about adverse health effects of long-term human exposure to ash from lava dome eruptions.

Volcanic ash is a potential hazard to human health, particularly on volcanoes that have long-lived eruptions, generate large amounts of fine ash, and where toxic forms of crystalline silica are an important component of the ash. Here we show that ash formed in the eruption of the Soufriere Hills volcano, Montserrat, contained significant amounts of respirable particles (that is, particles $< 3 \mu\text{m}$ in diameter, small enough to be deposited in the deep lung) and large amounts of cristobalite, an inhalation hazard that can cause silicosis. We discuss the mechanisms responsible and the possible hazards associated with the ash.

The Soufriere Hills volcano began erupting on 18 July 1995 (1). An andesite lava dome (58

to 60% SiO_2) extruded between 15 November 1995 and early March 1998 when growth ceased. Volcanic ash has been generated by two main mechanisms. First, collapse of parts of the unstable growing dome generated numerous pyroclastic flows and associated convecting plumes of fine ash. Second, vulcanian explosions produced large convecting ash plumes in two periods: 3 to 12 August 1997 and 21 September to 24 October 1997. Ash in vulcanian eruptions was generated both from eruption columns above the vent and from convective plumes associated with pumice flows.

The Soufriere Hills lava is a porphyritic andesite (35 to 45 weight % phenocrysts) that has varied little during the course of the eruption (2) (Table 1). The phenocryst assemblage consists of plagioclase, hornblende, orthopyroxene, titanomagnetite, and minor quartz (< 0.5 weight %). The groundmass consists of plagioclase, orthopyroxene, clinopyroxene, Fe-Ti oxides, glass, and silica minerals. The high-silica rhyolite glass content varies between about 25 to 30 weight % in rapidly erupted material to 5 to 15 weight % in slowly erupted lava. Groundmass silica phases (3 to 12 weight

%) occur in slowly erupted lava only, as vesicle infills, and as very fine-grained patches ($< 3 \mu\text{m}$) within interstitial glass. In contrast, pumice from explosive eruptions and rapidly erupted blocks of dome lava contain no free silica with the exception of sparse quartz phenocrysts. These observations suggest that the silica minerals in the lava are produced by vapor-phase crystallization and devitrification within the dome over periods of many days or weeks.

Fragmentation in pyroclastic flows produced by collapse of the lava dome generated large amounts of fine ash that formed buoyant plumes above the flow, rising to heights of several hundred meters to a few kilometers. The resulting fine ashfall deposits typically contain 60 to 70 weight % of 10- to 125- μm particles and 13 to 20 weight % of sub-10- μm particles. Ash samples from explosive vulcanian eruptions have bimodal grain size distributions, reflecting a mixture of coarser ash from the vulcanian explosions column and fine ash derived principally from the associated pumice flows. The vulcanian ashes contain less fine ash (30 to 35 weight %; 10 to 125 μm) and 13 to 14 weight % of sub-10- μm material.

We analyzed chemical compositions and the mineralogy of bulk and sub-10- μm ash samples by six methods: x-ray fluorescence (XRF), wet chemistry, electron probe microanalysis (EPMA), optical microscopy, x-ray diffraction (XRD), and ^{29}Si magic angle spinning nuclear magnetic resonance (MAS NMR) spectroscopy (3). We determined the compositions of the ash samples by XRF (Table 1). The content of free silica is determined by wet chemistry by the Talvite method (4), in which the sub-10- μm fraction is boiled in phosphoric acid to remove all minerals except for pure silica phases. Qualitative spectral analysis by EPMA (3) gave an estimate of the proportions of free silica. Agreement was good (usually within 3%) between the EPMA and Talvite methods (Table 2). In the sub-10- μm fractions of ash generated by pyroclastic flows related to dome collapse, the proportions of crystalline silica range between 10 to 24 weight % by EPMA and 10 to 27 weight % by the Talvite

¹ Department of Community Medicine, University of Cambridge, Gresham Road, Cambridge, CB12 5E, UK. ² Department of Earth Sciences, Bristol University, Queens Road, Bristol BS8 1RJ, UK. ³ Department of Physics, University of Warwick, Coventry CV4 7AL, UK. ⁴ British Geological Survey, Keyworth, Nottingham NG12 5GG, UK. ⁵ Institute of Occupational Medicine, 8 Roxburgh Place, Edinburgh EH8 9SU, UK.

*To whom correspondence should be addressed. E-mail: steve.sparks@bristol.ac.uk

method. Proportions of crystalline silica in explosively generated ash ranged between 4 to 6 weight % by EPMA and 5 to 6 weight % by the Talvite method.

Powder XRD and ²⁹Si NMR spectroscopy confirmed that the Talvite residues of the separated sub-10-μm ash contain only cristobalite, tridymite, and minor quartz. No amorphous or opaline silica is present (5). XRD (Fig. 1) was used to identify the polymorphs, and ²⁹Si MAS NMR allowed the relative abundances of different polymorphs to be determined. Sample H238 (Table 2), from an undisturbed site at the American School in Plymouth, 2.5 km west of the dome, represents the accumulation of many ashfall deposits between April 1996, when the first pyroclastic flows occurred, and May 1997. The silica residue was dominated by cristobalite (Figs. 1 and 2). In contrast, the residue of sample H239 from an ashfall on 30 March 1997 contained about 30% tridymite in addition to cristobalite. Both samples contained small amounts of quartz. Attempts to estimate the proportions of crystalline silica in the untreated sub-10-μm fractions of the same samples by ²⁹Si NMR spectroscopy were hindered by the presence of Fe in the glass. However, total crystalline silica contents in both samples were in excess of 15 weight %, consistent with results by EPMA and the Talvite method.

EPMA examination showed that the sub-10-μm fraction of both types of ash is strongly enriched in crystalline silica and glass relative to that of the magma and that mafic minerals are depleted. The sub-10-μm fraction of ash related to dome collapse pyroclastic flows is enriched in free silica (10 to 22 weight %) relative to dome samples (3 to 12 weight %). The smaller amounts of free silica in the sub-10-μm fraction of the vulcanian explosive ash (4 to 6 weight %) may represent incorporation of earlier erupted dome lava because the explosively erupted pumice contains <0.5 weight %

crystalline silica as quartz phenocrysts. Glass is the main constituent of the sub-10-μm fraction of both types of ash, along with plagioclase and minor amounts of mafic minerals forming the remainder, in addition to crystalline silica. The explosive ash typically contains higher proportions of glass (60 to 75 weight %) and lower proportions of plagioclase (14 to 25 weight %) in the sub-10-μm fraction than ash generated by pyroclastic flows, which contains between 30 to 60 weight % glass and 20 to 35 weight % plagioclase. These results show that crystalline silica is largely absent from magma erupted rapidly in explosions, but large amounts of crystalline silica form within the lava dome.

Ash samples generated by pyroclastic flows (Table 1) are enriched in SiO₂ and K₂O and depleted in TiO₂, FeO, MgO, and CaO relative to the magma. The sub-10-μm ash has even higher SiO₂ and K₂O contents (Table 1). Al₂O₃

contents decrease from magma to bulk ash and then increase in the sub-10-μm ash. In situ pyroclastic flow matrix (particles <4 mm in diameter) (Table 1) is depleted in SiO₂ and K₂O and enriched in TiO₂, FeO, MgO, CaO, and Al₂O₃. These variations can be explained by physical fractionation of components during magma fragmentation, caused by selective crushing of the weaker groundmass and preferential elutriation of fine particles into the ash plumes above pyroclastic flows. Phenocrysts of plagioclase and mafic minerals are preferentially retained in the pyroclastic flows (decreasing the Al₂O₃, TiO₂, FeO, MgO, and CaO content of the bulk ash). Glass, silica, and plagioclase microlites are preferentially crushed, enriching the sub-10-μm fraction in SiO₂, K₂O, and Al₂O₃ relative to the bulk ash. Mass balance calculations indicate that the silica polymorphs and glass are concentrated by factors of 2 to 5.

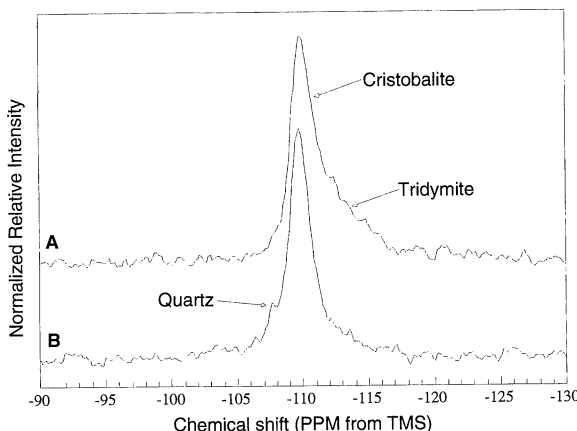


Fig. 2. ²⁹Si MAS NMR spectra of the residues from Talvite analysis of H239 (A) and H238 (B). The spectrum for H238 is dominated by a peak from cristobalite, whereas that for H239 shows additional intensity to the right of the main peak as a result of the presence of disordered tridymite. A very small peak for quartz can be detected in the spectrum for H238.

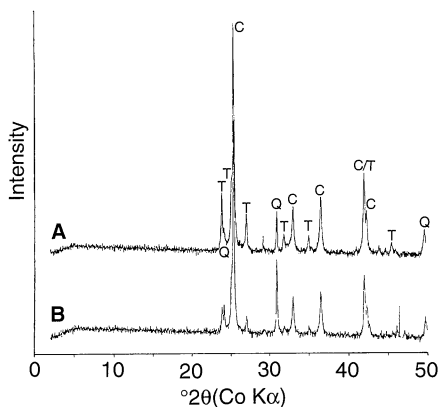


Fig. 1. Powder XRD patterns of the residues from Talvite analysis of H239 (A) and H238 (B). Cristobalite (C), tridymite (T), and minor quartz (Q) are the only phases present. H239 contains relatively more tridymite and less quartz than H238.

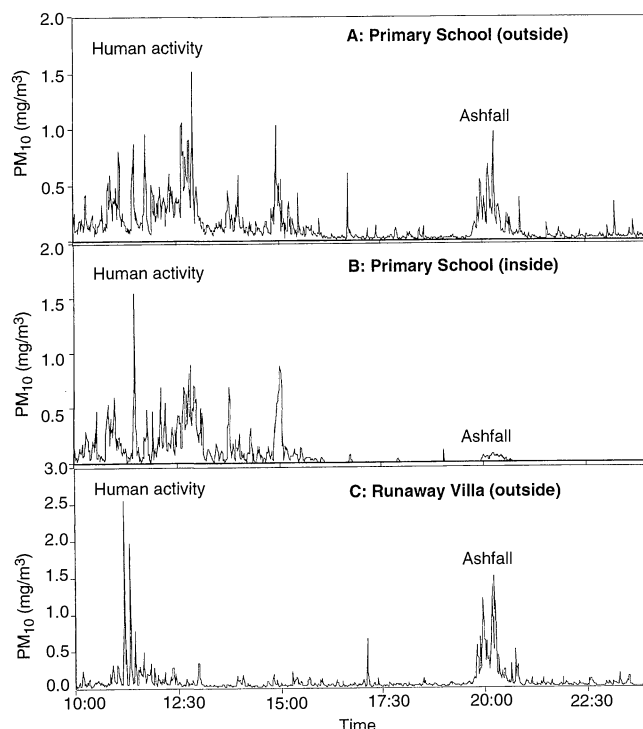


Fig. 3. Graphs comparing suspended fine ash (PM₁₀) trends over 14 hours on 10 October 1997 at three different sites. A vulcanian explosion at 18:40 produced ash fallout, shown by the peaks around 20:00. Human activity can produce higher PM₁₀ values than normal ashfall. At the Primary School (A and B), the highest PM₁₀ values were recorded during break periods and at 15:00 when the children leave school. Values inside and outside are comparable during the morning, but are much lower inside (0.03 mg/m³) than outside (0.27 mg/m³) after 15:00. At Runaway Villa (C), morning housework activities (sweeping) produce higher peaks than the evening ashfall.

Table 1. Whole-rock analyses of andesite and ash (XRF) and of groundmass glass (EPMA). Total iron (FeO^T) is calculated as FeO, and all analyses are normalized to 100% volatile free. Column 2 gives an average magma composition. Columns 3 to 6 are average bulk and sub-10-μm ash compositions from pyroclastic flows (PF) and explosive eruptions (Ex). The pyroclastic flow matrix (column 7) represents the complement of ash elutriated from the pyroclastic flows. Column 8 gives an average groundmass glass. The number of analyses for each sample is given in parentheses.

Sample	Andesite (22)	Bulk ash PF-fall (15)	<10 μm PF-fall (5)	Bulk Ex-fall (5)	<10 μm Ex-fall (4)	PF matrix (1)	Gms glass (8)
SiO ₂	59.48	64.66	67.39	60.80	69.84	57.88	77.87
TiO ₂	0.64	0.51	0.24	0.58	0.33	0.67	0.38
Al ₂ O ₃	18.02	16.23	16.69	18.04	14.60	18.24	11.48
FeO ^T	6.72	5.47	3.29	6.08	3.47	7.22	2.02
MnO	0.18	0.16	0.11	0.16	0.11	0.21	0.13
MgO	3.00	2.24	1.54	2.49	1.51	3.25	0.31
CaO	7.61	5.91	4.66	7.29	4.20	8.04	1.81
Na ₂ O	3.49	3.63	4.44	3.55	4.13	3.64	3.62
K ₂ O	0.73	1.04	1.48	0.86	1.69	0.70	2.27
P ₂ O ₅	0.15	0.14	0.15	0.14	0.10	0.15	0.11

Selective crushing and enrichment of glass in the ashfall components of pyroclastic flows have been widely recognized (6). In contrast, the composition of explosion-generated bulk ash differs only slightly from that of the magma. The same elements are slightly enriched and depleted in the ash generated from dome-collapse pyroclastic flows. However, the sub-10-μm fraction of the explosive ash had even higher SiO₂ and K₂O and lower Al₂O₃ contents than the same fraction of the collapse-generated ash because of higher glass and lower plagioclase contents in the former. Glass is enriched in the sub-10-μm fraction of the explosive ash by a factor of 2 to 4 relative to the magma.

Concentrations of airborne respirable dust (≤3 μm in diameter) and PM₁₀ (≤10 μm diameter) have been monitored around the volcano with Dust Trak monitors and cyclone samplers (7), combined with gravimetric and XRD analysis (8). Airborne ash concentrations (PM₁₀) have been continually monitored since

Table 2. Comparison of total crystalline silica contents of the sub-10-μm fraction of several ash samples through the use of grain counting by EPMA and the Talvite dissolution method. The EPMA grain count data are corrected to weight % with density values of 2.3 for glass and silica (predominantly cristobalite). Ash associated with collapse-generated pyroclastic flows (PF) has significantly higher values of crystalline silica than ash from vulcanian explosions (VE).

Sample number	Eruption mode	EPMA (wt %)	Talvite (wt %)
H238	*	17.5	15.2
H239	PF	21.9	27.0
H334	PF	17.1	16.2
H420	PF	10.5	10.4
H416	VE	3.9	6.1
H417	VE	4.7	5.2
H421	VE	5.6	5.6

*Sample H238 was collected from an undisturbed horizon in May 1997 and represents an accumulation of ash, generated predominantly by pyroclastic flows, covering the entire eruption up to that time.

August 1997 at five fixed stations and by roving studies at sites where there is significant human activity. Environmental concentrations of ash have regularly exceeded the UK air quality standard (9) for PM₁₀ (50 μg/m³, 24-hour rolling average) in areas subject to frequent ashfall. Outdoor occupational exposures to cristobalite were measured with personal cyclone samplers, and the levels sometimes exceeded the American Conference of Government Industrial Hygienists threshold limit value (0.05 mg/m³ averaged over an 8-hour workday) (10). The mean exposures of people living in Cork hill, before evacuation, also exceeded this limit after adjusting for 24 hours of exposure every day of the week. Exposure of the population to ash partly depends on the wind. Most ash plumes are blown to the west by low-altitude winds so that Plymouth has had the greatest ash deposition. High-level winds (above 4- to 6-km altitude) are commonly from the southeast and infrequently from the south. Thus, populated areas in the center of the island have received significant ashfall, whereas northern Montserrat has received only light ashfall. Rain removes airborne dust and dampens deposited ash, reducing the potential for resuspension. The areas in Montserrat most susceptible to the ash hazard are now evacuated.

Human activity is a significant factor in determining exposure. Our roving studies in areas of different kinds of human activity consistently show increased concentrations of airborne dust whenever there was human activity. For example, the primary school (Fig. 3) airborne dust levels were higher during the school day and peaked at lunch break. The only ashfall of that day occurred in the late afternoon and had less effect on airborne dust concentrations than the children's activity. Concentrations of PM₁₀ were high in car parks, busy roads, supermarkets, and in occupied houses, as a result of human activities. Morning sweeping in occupied houses, for example, raised suspended ash concentra-

tions (Fig. 3). Field observations and scanning electron microscopy studies show that ash falls in clusters and that much of PM₁₀ is locked in these clusters during primary fallout (11). It is surmised that clusters break down by reworking after deposition, accounting for the large effects of human activity on airborne dust concentrations.

This study suggests that there is a potential health threat from long-term exposure to volcanic ash generated by pyroclastic flows from lava domes. Exposure to crystalline silica can lead to the development of silicosis, which is an irreversible scarring disease of the lungs. Some types of crystalline silica are classified as a human carcinogen by the International Agency for Research on Cancer (12), and cristobalite is thought to be more harmful than quartz (13). In the 1980 eruptions of Mount St. Helens, USA, sub-10-μm particles accounted for about 10 weight % of the ash (14, 15). Samples of sub-10-μm ash contained 4 weight % cristobalite and 3 weight % quartz. Exposures in the affected communities were of limited duration, because ashfalls soon ceased, and the risk of silicosis was considered insignificant (14, 15). The hazard is much greater during long-lived eruptions such as at the Soufriere Hills volcano, which are characterized by persistent ashfall over many months or years. The hazard is also increased in dome eruptions because of production of fine ash, the formation of crystalline silica in the dome, and its concentration in fine ash generated from dome-collapse pyroclastic flows by selective crushing. In contrast, explosively erupted ash contains lower quantities of crystalline silica than ash produced by pyroclastic flows generated by collapse of the lava dome.

References and Notes

1. S. R. Young *et al.*, *Geophys. Res. Lett.* **25**, 3389 (1998).
2. M. D. Murphy *et al.*, *ibid.*, p. 3433.
3. XRD was performed with a Phillips PW1700 diffractometer by using Co-Kα radiation generated at 45 kV and 40 mA, a step size of 0.02° 2θ, and sampling time of 1.5 s per step. A zero background Si substrate was used, and the sample was mounted by using a drop of acetone. NMR spectra were collected with a Bruker MSL 360 operating at 71.535 MHz with a 2-μs pulse length and 180-s recycle delay. Samples were analyzed on a JEOL JXA-8600 electron microprobe by energy-dispersive spectral analysis to identify the phases. Run conditions were 15-kV accelerating voltage, 15-nA beam current, and 1-μm probe diameter. The proportions of different phases in the sub-10-μm fraction were estimated by counting 200 grains per sample.
4. N. A. Talvite, *Am. Ind. Hydrol. Assoc. J.* **25**, 169 (1964).
5. Opaline silica typically can be identified as a broad peak on XRD, but our XRD traces show no evidence of its presence (Fig. 1). Opaline silica is also formed in low-temperature environments and would not be expected in a high-temperature lava dome.
6. R. L. Hay, *J. Geol.* **67**, 540 (1959); G. P. L. Walker, *Contrib. Mineral. Petrol.* **36**, 135 (1972); R. S. J. Sparks and G. P. L. Walker, *J. Volcanol. Geotherm. Res.* **2**, 329 (1997).

REPORTS

7. Health and Safety Executive (UK), *Methods for the Determination of Hazardous Substances* **14/2** (1997).
8. ———, *ibid.* **76** (1994).
9. Expert Panel on Air Quality Standards, *Particles* (Department of the Environment Expert Panel for Air Quality Standards, Her Majesty's Government, 1995).
10. Health and Safety Executive, *Occupational Exposure Limits* **EH40/97** (1997); *American Conference of Government Hygienists, Threshold Limit Values for Chemical Substances and Physical Agents: Biological Exposure Indices* (American Conference of Government Hygienists, Cincinnati, OH, 1997).
11. R. K. Soren, *J. Volcanol. Geotherm. Res.* **13**, 63 (1982).
12. World Health Organization, *Monographs on the Evaluation of Carcinogenic Risks to Humans* **68** (1997).
13. P. J. Heaney and J. A. Banfield, in G. D. Guthrie and B. T. Mossman, Eds., *Rev. Mineral. Min. Soc. Am.* **28**, 185 (1993).
14. D. D. Dollberg, M. L. Bolyard, D. L. Smith, *Am. J. Public Health* **76** (suppl.), 53 (1986).
15. A. S. Buist, R. S. Bernstein, L. R. Johnson, W. M. Vollmer, *ibid.*, p. 66.
16. Work on Montserrat was supported by the Department for International Development and Natural Environmental Research Council. The cooperation of the people of Montserrat and staff of the Montserrat Volcano Observatory is acknowledged. We thank T. S. Brewer (Leicester University) for performing XRF analyses of lava samples, T. Riemer and B. Schmidt (Warwick University) for performing NMR experiments, and A. Seaton (Aberdeen University) for advice.

23 October 1998; accepted 15 January 1999

Supertetrahedral Sulfide Crystals with Giant Cavities and Channels

Hailian Li, Aaron Laine, M. O'Keeffe,* O. M. Yaghi*

Although aluminosilicates and metal phosphates can form porous open-framework materials such as zeolites, sulfide analogs usually form high-density phases because of the relatively small tetrahedral angle at sulfur atoms. One strategy to overcome this limitation is to use tetrahedral clusters as the building blocks to achieve porous sulfide-based networks. The preparation and crystal structures of two indium sulfide open frameworks (ASU-31 and ASU-32) built of supertetrahedral clusters around organic template and water guests are described. ASU-31, based on the sodalite-tetrahedrite network, contains cavities 25.6 angstroms in diameter, and ASU-32, based on the tetragonal CrB_4 network, contains channels with a minimum diameter of 14.7 angstroms. The organic cations can be completely exchanged with sodium ions in aqueous solution at room temperature without degradation of the crystals.

The intense pursuit of open crystalline assemblies extends across the gamut of organic and inorganic compositions (1) and is motivated by the interest in creating structures with cavities and channels that may be exploited in nanotechnology, including shape- and size-selective catalysis, separations, sensors, and optoelectronic and molecular recognition applications. Until recently the largest cavities known in crystalline solids were those in oxide zeolites (2), discussed further below, although a cubic organic crystal with a very large cavity volume has been described (3). Here we use a design strategy for production of materials with even larger cavities and show its implementation in the synthesis of indium sulfide framework structures.

Chalcogenide-based systems should be a fruitful source of porous materials (4–7), but when TO_4 tetrahedra in oxide frameworks (where T is an atom supporting tetrahedral coordination) are replaced by TS_4 tetrahedra, the frameworks tend to contract to higher density because of the smaller T-S-T angles compared with T-O-T angles. Thus the well-known low-

density cristobalite framework of SiO_2 (with Si atoms on a diamond net) contracts to denser structures with close-packed anions (8, 9) in sulfide materials such as chalcopyrite (CuFeS_2) (8). One strategy for making more open structures, and it is the one that we consider here, is

to replace TS_4 units with tetrahedral clusters or supertetrahedra such as the T2 and T3 units containing 4 and 10 tetrahedra, respectively (9–11) (Fig. 1). Cristobalite topology structures with all T2 units have long been known as the ZnI_2 structure (9). However, in these structures, two contracted frameworks interpenetrate and the anion arrangement is again close-packed—indeed, GeS_2 with this structure (12) is actually the densest of all four known ambient-pressure polymorphs. Nevertheless, a number of more open structures based on T2 units have been described (13, 14). A structure, that of $\text{Ag}_6\text{B}_{10}\text{S}_{18}$, with T3 units has also been known for some time (15) but the framework of corner-connected supertetrahedra, although unusual, is very dense. More recently, a cristobalite-framework compound with T3 InS clusters and including dimethylamine has been reported (16); in this material, there are again two interpenetrating diamond nets and the structure does not contain large cavities (17). The same is true for the “double diamond” sulfide compound built up from approximately tetrahedral clusters containing 17 Cd atoms (18) and for a T3 Sn-O-S compound (19).

To make very open tetrahedral sulfide materials, three conditions should be met: (i) the

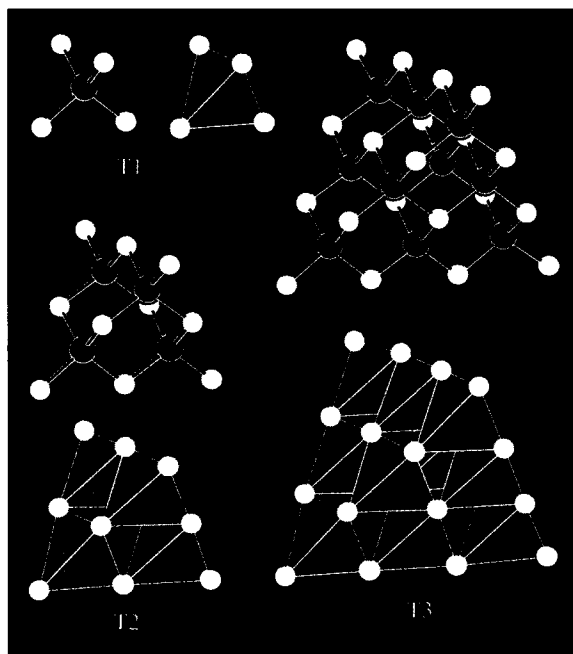


Fig. 1. The first three of the supertetrahedron family T_n . The T3 tetrahedron shown is the real one from the crystal structure of ASU-31 described here (stick-and-ball: In, red; S, yellow; polyhedra: In, blue; S, yellow).

Supramolecular Design and Discovery Group, Department of Chemistry and Biochemistry, Arizona State University, Tempe, AZ 85287, USA.

*To whom correspondence should be addressed. E-mail: mokeeffe@asu.edu and oyaghi@asu.edu